

# Temperature-dependent Raman study of multiferroic $\text{Bi}_2\text{NiMnO}_6$ thin films

M. N. Iliev,<sup>1</sup> P. Padhan,<sup>2</sup> and A. Gupta<sup>2</sup><sup>1</sup>Texas Center for Superconductivity and Department of Physics, University of Houston, Houston, Texas 77204-5002, USA<sup>2</sup>Center for Materials for Information Technology and Department of Chemistry, University of Alabama, Tuscaloosa, Alabama 35487, USA

(Received 9 March 2008; revised manuscript received 29 April 2008; published 20 May 2008)

The Raman spectra of  $\text{Bi}_2\text{CoMnO}_6$  (BNMO) thin films, grown on (001)- $\text{SrTiO}_3$ , (001)- $\text{NdGaO}_3$  (NGO), and (110)- $\text{DyScO}_3$  substrates, have been measured in the temperature range 80–700 K. The spectra are similar to those of  $\text{La}_2\text{NiMnO}_6$  and  $\text{La}_2\text{CoMnO}_6$ , the position of the main peak at 610–620  $\text{cm}^{-1}$  being sensitive to the type of substrate. The softening below 140 K and a steplike anomaly at 420–490 K of the main Raman peak frequency provide strong evidence that the structural, magnetic, and ferroelectric properties of the BNMO/NGO films are similar to those of the bulk material.

DOI: [10.1103/PhysRevB.77.172303](https://doi.org/10.1103/PhysRevB.77.172303)

PACS number(s): 78.30.-j, 75.47.Lx, 63.22.-m

## I. INTRODUCTION

In the search for magnetoelectric coupling effects at higher temperatures, there have been recent efforts devoted to the study of ferromagnetic double perovskites  $R_2\text{AMnO}_6$  ( $R$ =rare earth;  $A$ =divalent metal).<sup>1–7</sup> Although materials such as  $\text{La}_2\text{NiMnO}_6$  (LNMO) and  $\text{La}_2\text{CoMnO}_6$  (LCMO) ferromagnetically order at relatively high temperatures ( $T_{\text{CM}} \approx 280$  and 230 K, respectively), they do not possess ferroelectric orders and cannot be considered as true multiferroics. Recently, the coexistence of ferromagnetic ( $T_{\text{CM}}=140$  K) and ferroelectric ( $T_{\text{CE}}=485$  K) orders has been reported for the strongly distorted  $\text{Bi}_2\text{NiMnO}_6$  (BNMO), prepared in the bulk by high pressure synthesis<sup>8</sup> and, subsequently, as thin films on the  $\text{SrTiO}_3$  substrate by pulsed laser deposition.<sup>9</sup> The  $B$ -site ordering in the films has been confirmed by synchrotron x-ray diffraction.<sup>10</sup> Predictions of the crystallographic and electronic structures of BNMO and related magnetic and ferroelectric properties based on first-principles calculations have also been reported.<sup>11</sup>

In this Brief Report, we report the results of a Raman study of BNMO thin films deposited on different substrates [ $\text{SrTiO}_3$ (STO),  $\text{DyScO}_3$ (DSO), or  $\text{NdGaO}_3$ (NGO)] and discuss them in close comparison to similar studies of LNMO<sup>12</sup> and LCMO.<sup>13</sup> The variation with temperature of the main Raman peak, studied in detail for the BNMO/NGO film between 80 and 700 K, exhibits anomalies close to  $T_{\text{CM}}$  and  $T_{\text{CE}}$  of the bulk sample.<sup>8</sup>

## II. SAMPLES AND EXPERIMENT

Pulsed laser deposition was used to grow epitaxial thin films (20–50 nm) of BNMO on (001)-oriented STO and NGO, and (110)-oriented DSO substrates at 700 °C in oxygen ambient of 800 mTorr. The films were subsequently annealed for 1 h at 470 °C in 760 Torr oxygen pressure before cooling down to room temperature. The crystalline quality of the samples was analyzed using a Philips X'Pert x-ray diffraction (XRD) system. Only the pseudocubic (00 $l$ ) reflections of the BNMO film and substrate were observed in the  $\theta$ – $2\theta$  x-ray scans. The effect of substrate-induced strain was

clearly reflected in the angular position of the BNMO peaks, which yielded strained out-of-plane pseudocubic lattice parameters for BNMO of 3.857, 3.865, and 3.889 Å on STO, NGO, and DSO, respectively. All of the films exhibited a fourfold symmetry in the  $\phi$  scan of the asymmetric plane, consistent with epitaxial growth.

Magnetization ( $M$ ) versus temperature ( $T$ ) was measured using a Quantum Design superconducting quantum interference device magnetometer. For a 32-nm-thick BNMO film on STO, the  $M(T)$  curve showed ferromagnetic ordering below a Curie temperature of  $T_{\text{CM}} \approx 130$  K, which is slightly lower than the bulk value of 140 K.

The Raman spectra between 80 and 700 K were measured in the backward scattering configuration using a triple Raman spectrometer (T64000) equipped with a microscope, an optical cryostat, a heating stage, and a liquid nitrogen cooled charge coupled device camera. To avoid local heating, the laser power density was kept below  $10^4$  W/cm<sup>2</sup>. As a rule, the experimental spectra also contained contributions due to scattering from the substrate—its relative intensity being dependent on the film thickness, the excitation laser line wavelength (633, 515, 488, or 458 nm), and the microscope objective (50 $\times$  or 100 $\times$ ) used. To obtain the pure BNMO spectra, at each temperature, the Raman spectrum of the substrate was also measured in the same scattering configuration and subtracted from the pristine spectrum using the GRAMS software. The same software was used to fit the line shape of the pure BNMO spectra and obtain the Raman line parameters.

## III. RESULTS AND DISCUSSION

Figure 1 shows the polarized spectra of BNMO films deposited on (001)-NGO, (001)-STO, and (110)-DSO substrates, as obtained with parallel (HH) polarizations of the incident and scattered light. The corresponding spectra of LCMO and LNMO are also shown for comparison. All spectra are dominated by two main spectral features: (1) a high frequency band that peaks in the 600–670  $\text{cm}^{-1}$  range, pronounced much more strongly with parallel polarization of the incident and scattered light; (2) a broader band at a lower frequency (460–540  $\text{cm}^{-1}$ ), which can exhibit a complex

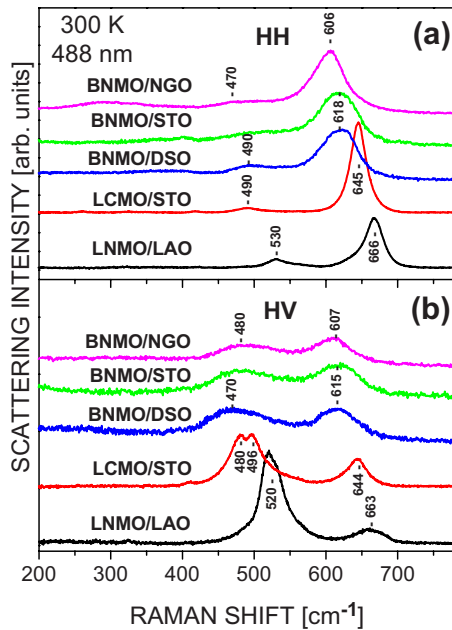


FIG. 1. (Color online) Comparison of the Raman spectra of BNMO/NGO, BNMO/STO, BNMO/DSO, LCMO/STO, and LNMO/LAO as obtained with 488 nm excitation at 300 K. H and V denote two orthogonal directions rotated by  $45^\circ$  with respect to the Mn-O-Ni/Co chains. The spectra are vertically shifted for clarity. The HV vertical scale is enlarged by a factor of 3 compared to that of the HH spectra.

structure, being as a rule of comparable intensity for the crossed and parallel scattering configurations. The detailed analysis of these spectral structures in the case of LCMO<sup>13</sup> and LNMO<sup>12</sup> has shown that the high frequency band corresponds to stretching (“breathing”) vibrations of the Ni(Co)/MnO<sub>6</sub> octahedra, whereas the lower lying complex band is in the frequency range of antistretching and bending motions.

Although at 300 K, the structures of LCMO/LNMO ( $P2_1/n$ ) and BNMO ( $C2$ ) are different (see Fig. 2), the similarity of the spectral profiles is not unexpected since both the stretching (S) and antistretching (AS) modes originate from the Raman allowed modes ( $A_{1g}$  and  $E_g$ ) of the idealized undistorted  $Fm3m$  parent structure and the monoclinic distortions of the  $P2_1/n$  and  $C2$  phases will only have a modest effect on the mode frequency and relative intensity. This is confirmed by the fact that the profile of the Raman spectra of BNMO is practically insensitive to the  $P2_1/n \rightleftharpoons C2$  structural transition at  $\approx 458$  K (Fig. 3).

The decrease in the stretching mode frequency in the LNMO-LCMO-BNMO sequence can be qualitatively explained by the increase in the averaged B-O bond length ( $B=\text{Ni,Co,Mn}$ ) from 1.963 Å in LNMO<sup>2</sup> to 1.978 Å in LCMO<sup>2</sup> and 1.994 Å in BNMO.<sup>8</sup> These bond length values, however, would be somewhat different in the case of thin films due to the strain resulting from the film-substrate lattice mismatch. This explains the variation in the main Raman band position in BNMO/NGO, BNMO/STO, and BNMO/DSO, illustrated in Fig. 1.

In order to investigate the effects of the magnetic and structural transitions on the Raman phonon parameters in

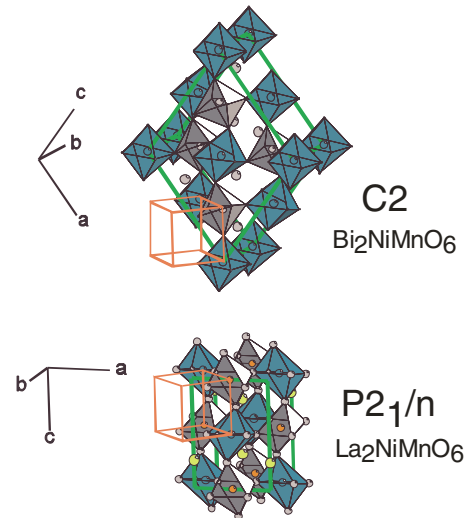


FIG. 2. (Color online) Comparison of the crystal structures of  $\text{Bi}_2\text{NiMnO}_6$  ( $C2$ ) and  $\text{La}_2\text{NiMnO}_6$  ( $P2_1/n$ ). The ideal perovskite unit cell is also shown.

BNMO, we have collected more than 30 spectra from the same spot on the BNMO/NGO thin film at various temperatures between 80 and 700 K. The spectral profiles have been fitted by three pure Lorentzians or three mixed Lorentzian-Gaussian curves centered near 315, 495, and 610  $\text{cm}^{-1}$ . The parameters of the curve centered near 610  $\text{cm}^{-1}$  turn out to be practically the same for the two types of fitting profiles. Figure 4 shows the variation with temperature of the center and width of this band.

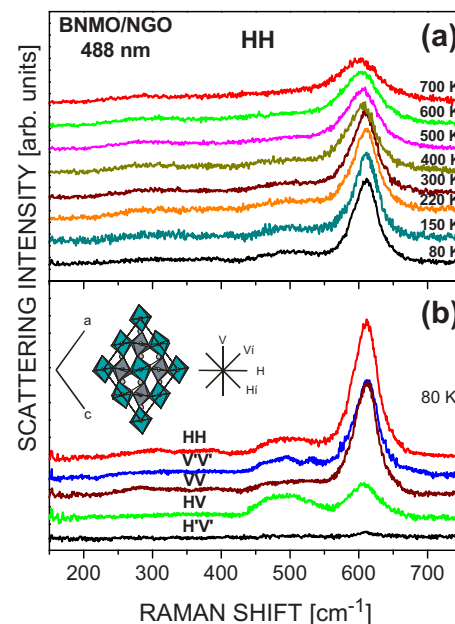


FIG. 3. (Color online) (a) Temperature dependence of the Raman spectra of BNMO/NGO between 80 and 700 K; (b) polarized Raman spectra of BNMO/NGO at 80 K. The first and second letters denote, respectively, the polarization directions of the incident and scattered light. In this experiment, H and V are along the [010] and [100] directions of the NGO substrate.

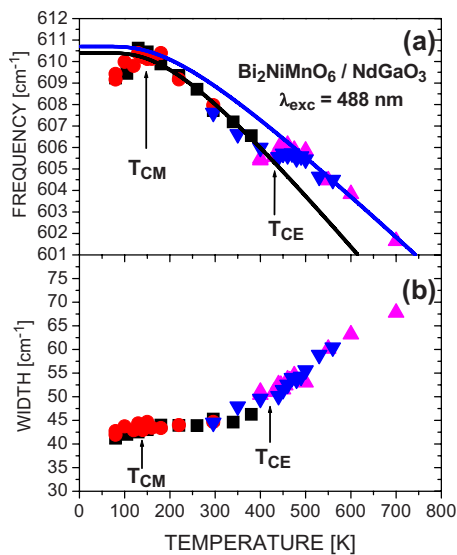


FIG. 4. (Color online) Variation with temperature of the position and width of the Raman peak of the BNMO/NGO thin film. The different symbols correspond to different sets of measurements performed on four consecutive days. The curves correspond to the standard  $\omega_{\text{anh}}(T)$  dependence due to anharmonic phonon-phonon scattering.

In general, the change  $\Delta\omega(T)$  in phonon frequency with temperature is a sum of several contributions due to: (i) anharmonic scattering ( $\Delta\omega_{\text{anh}}$ ), (ii) spin-phonon coupling ( $\Delta\omega_{\text{s-ph}}$ ), (iii) lattice expansion and/or contraction ( $\Delta\omega_{\text{latt}}$ ), and (iv) phonon renormalization ( $\Delta\omega_{\text{ren}}$ ) resulting from electron-phonon coupling.<sup>14</sup> Given that BNMO is a ferroelectric material, the carrier concentration is low and the last term  $\Delta\omega_{\text{ren}}$  can be neglected. The contributions of  $\Delta\omega_{\text{s-ph}}$  and

$\Delta\omega_{\text{latt}}$  have to be pronounced mostly below  $T_{\text{CM}}$  and near  $T_{\text{CE}}$ , respectively. Above  $T_{\text{CM}}$  and far from  $T_{\text{CE}}$ ,  $\omega(T)$  is expected to be governed by the anharmonic phonon-phonon scattering following the dependence  $\omega_{\text{anh}}(T) = \omega_0 - C(1 + \frac{2}{e^{\hbar\omega/2kT} - 1})$ , where  $\omega_0$  and  $C$  are adjustable parameters. As seen in Fig. 4, the experimental points between 140 and 420 K, and above 490 K, respectively, are close to two  $\omega_{\text{anh}}(T)$  dependences characterized by different  $\omega_0$  and  $C$ , which points to the existence of a structural transition between 420 and 490 K. This is consistent with the observation of a structural transition at 485 K in bulk BNMO.<sup>8</sup> Another visible anomaly in the experimental  $\omega(T)$  dependence is the deviation from  $\omega_{\text{anh}}(T)$  toward lower frequencies for  $T < 140$  K. Such phonon softening below the ferromagnetic ordering temperature has already been reported for LCMO<sup>13</sup> and LNMO,<sup>12</sup> as well as for A-type antiferromagnets  $\text{RMnO}_3$  ( $R = \text{La, Pr, Nd, Sm}$ )<sup>14,15</sup> and has been ascribed to magnetic-order-induced phonon renormalization.

In conclusion, despite some structural differences between  $\text{Bi}_2\text{NiMnO}_6$ ,  $\text{La}_2\text{NiMnO}_6$ , and  $\text{La}_2\text{CoMnO}_6$ , their Raman spectra exhibit definite similarities. The softening below 140 K and a steplike anomaly at 420–490 K of the main Raman peak frequency provide strong evidence that the structural, magnetic, and ferroelectric properties of the BNMO/NGO films are close to those of the bulk material.

#### ACKNOWLEDGMENTS

This work was supported in part by the State of Texas through the Texas Center for Superconductivity at the University of Houston (TcSUH) and by Grant No. TK-X-1712/2007 of the Bulgarian Science Fund. The work at the University of Alabama was supported by ONR Grant No. N000140610226.

- <sup>1</sup>N. S. Rogado, J. Li, A. W. Sleight, and M. A. Subramanian, *Adv. Mater.* (Weinheim, Ger.) **17**, 2225 (2005).
- <sup>2</sup>C. L. Bull, D. Gleeson, and K. S. Knight, *J. Phys.: Condens. Matter* **15**, 4927 (2003).
- <sup>3</sup>R. I. Dass and J. B. Goodenough, *Phys. Rev. B* **67**, 014401 (2003).
- <sup>4</sup>R. I. Dass, J.-Q. Yan, and J. B. Goodenough, *Phys. Rev. B* **68**, 064415 (2003).
- <sup>5</sup>H. Guo, J. Burgess, S. Steet, A. Gupta, T. G. Calvarese, and M. A. Subramanian, *Appl. Phys. Lett.* **89**, 022509 (2006).
- <sup>6</sup>M. Hashisaka, D. Kan, A. Masuno, M. Takano, Y. Shimakawa, T. Terashima, and K. Mibu, *Appl. Phys. Lett.* **89**, 032504 (2006).
- <sup>7</sup>C. L. Bull and P. F. McMillan, *J. Solid State Chem.* **177**, 2323 (2004).
- <sup>8</sup>M. Azuma, K. Takata, T. Saito, Sh. Ishiwata, Y. Shimakawa, and M. Takano, *J. Am. Chem. Soc.* **127**, 8889 (2005).

- <sup>9</sup>M. Sakai, A. Masuno, D. Kan, M. Hashisaka, K. Takata, M. Azuma, M. Takano, and Y. Shimakawa, *Appl. Phys. Lett.* **90**, 072903 (2007).
- <sup>10</sup>Y. Shimakawa, D. Kan, M. Kawai, M. Sakai, S. Inoue, M. Azuma, S. Kimura, and O. Sakata, *Jpn. J. Appl. Phys., Part 2* **46**, L845 (2007).
- <sup>11</sup>A. Ciucivara, B. R. Sahu, and L. Kleinman, *Phys. Rev. B* **76**, 064412 (2007).
- <sup>12</sup>M. N. Iliev, H. Guo, and A. Gupta, *Appl. Phys. Lett.* **90**, 151914 (2007).
- <sup>13</sup>M. N. Iliev, M. V. Abrashev, A. P. Litvinchuk, V. G. Hadjiev, H. Guo, and A. Gupta, *Phys. Rev. B* **75**, 104118 (2007).
- <sup>14</sup>E. Granado, A. García, J. A. Sanjurjo, C. Rettori, I. Torriani, F. Prado, R. D. Sánchez, A. Caneiro, and S. B. Oseroff, *Phys. Rev. B* **60**, 11879 (1999).
- <sup>15</sup>J. Laverdière, S. Jandl, A. A. Mukhin, V. Yu. Ivanov, V. G. Ivanov, and M. N. Iliev, *Phys. Rev. B* **73**, 214301 (2006).